

# Effect of Initial Crack Length of C(T) Specimen on Crack Propagation Measurement by Dc Potential Drop Method

Ni Chenqiang, Xue He<sup>\*</sup> and Wang Weibing

School of Mechanical Engineering, Xi'an University of Science and Technology,  
Xi'an 710054, China

\*

xuehe1961@163.com

**Abstract.** The compact tensile specimens (C(T) specimens) are commonly used in crack propagation tests. The DC potential drop method is an important method for measuring crack length in crack propagation tests. To investigate the influence of the initial crack length of the C(T) specimen on the calibration curve in practice, the variation law of the potential field distribution of the compact tensile specimen with the crack propagation has been studied. The measurement features in different initial crack lengths and different current injection positions were quantitatively analyzed. The results show that the initial crack length has a significant effect on the sensitivity of the signal and the linearity of the calibration curve. The sensitivity can be improved by increasing the initial crack length, while the linearity decrease.

## 1. Introduction

Compact tensile specimens (C(T) specimens) are commonly used for establishing crack growth rate models, determining creep fracture properties, and determining fracture toughness of materials through experimental methods [1,2]. When it was used for the crack propagation test, the crack growth rate was obtained by measuring the amount of crack propagation in the test [3,4]. There are several methods that can be used to achieve online crack monitoring, while in the closed environment that crack cannot be directly observed the DC potential drop method is the most commonly used method to achieve long-term monitoring during the crack propagation [5]. The principle of the DC potential drop method is to pass a constant DC current on the cracked metal specimen, and measure the crack length by measuring the potential difference at a specific location of the specimen [6]. Since conductivity of metals is very excellent, the output signal of the potential drop method is very small. So the accurate calibration of the crack length and the potential difference curve is a very important. For the case of an infinitely long, limited-width center cracked plate specimen with a constant current perpendicular to the crack plane, Johnson gave the relationship between potential difference and crack length [7], which is called Johnson's formula. Afterward, the potential field of the bending specimen and the simplified compact tensile specimen (C(T) specimen) was analyzed [8]. For the three-dimensional potential field distribution of cracked specimens, the finite element method is generally used [9]. However, since the shape of the C(T) specimen is quite different from the model used in the above study, none of the above analytical solutions could be applied. According to the standard test method for linear-elastic plane-strain fracture toughness[10], the initial crack length of the specimen is counted from the pin hole, but this standard does not give its selection basis. Compared with the analytical model, a considerable part of the "crack" of a C(T) specimen is a slot, whose width is much larger than the width of the crack. So the initial crack length will significantly affect the geometry of the



specimen and thus affect its equivalent resistance. In this paper, the finite element software is used to analyze the three-dimensional potential field of CT specimens, and the influence of different initial crack lengths on the calibration curve is studied. Quantitative analysis is also provided to give a basis for practical application of crack measurement based DC potential drop method.

**2. Finite Element Model**

The geometry of the C(T) specimen, which is in accordance with ASTM E399-09 [10], is shown in Figure. 1. The nominal width of the specimen  $W=25\text{mm}$ , the specimen thickness  $B=0.5W$ . A 3D 1/4 finite element model of the specimen was developed using a commercial FEM software. Since the geometry of the specimen is symmetrical to the crack plane and the current injection points are symmetrical to the crack plane in practice, it is enough to develop a 1/4 finite element model (take half of the specimen on one side of the crack plane and take half the thickness of the specimen). Cracks were simulated using a rectangular slot with a width of 0.01 mm. The specimen grid model is shown in Figure. 2. The mesh near the crack was refined to ensure calculation accuracy.

To simulate a constant current flow through the specimen, a point source unit current (1A) was applied to the current injection point. According to symmetry, the ligament ahead of the crack tip is a uniform potential surface, so a ground (0 V potential) boundary condition was applied to the ligament ahead of the crack tip. For material properties, only the conductivity of the material is required, and it was set to 1388.89 S /mm [9], the conductivity of 304 stainless steel commonly used in structural materials for pressure vessels in nuclear power plants.

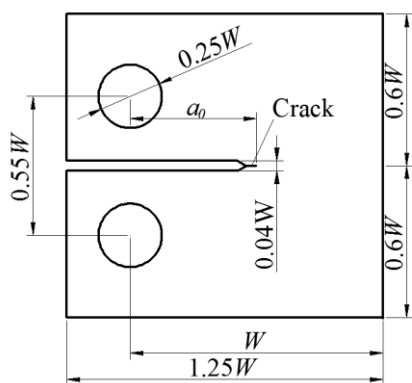


**Figure 1.** Geometry of C(T) specimen

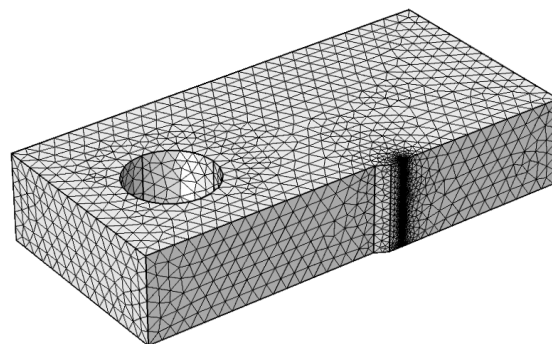


**Figure 2.** Finite element mesh of C(T) specimen model

**3. Results and Discussion**

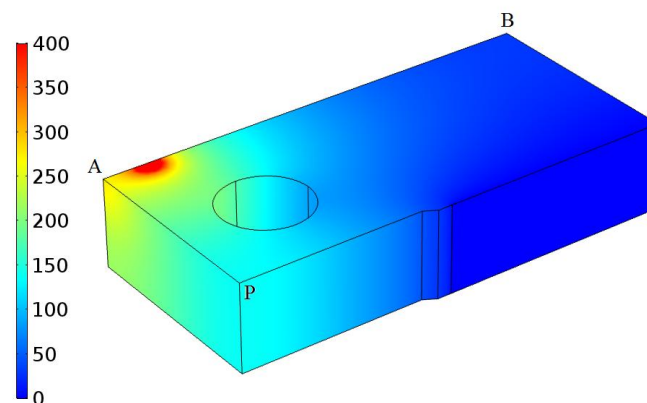


**Figure 3.** The potential( $\mu\text{V}$ ) distribution at  $a/W=0.35$

An example of the potential distribution (current is input near the upper left corner of the specimen, at  $a/W=0.35$ ) is shown in Figure. 3. With the software post-processing function, the potential of any point in the three-dimensional space of the specimen under different initial crack lengths, different potential loading positions and different crack length increments can be obtained. Because the current injection position has a significant influence on the potential field distribution, the potential fields under different current injection positions are calculated separately. All the studied current injection points is selected on the intersection line between the top surface of the specimen and the plane perpendicular to the middle plane of the thickness direction (ie, the line AB in Figure. 3), and the symbol  $LP$  ( $0 \leq LP \leq 1$ ) represents different positions from left to right. The potential difference signal is measured from the notch mouth (point P in Figure. 3).

### 3.1. Sensitivity

Figure. 4 (a) and (b) show the average sensitivity of the potential difference signals corresponding to different initial crack lengths  $a_0$  for two crack extension ranges. As can be seen from the figures, the signal sensitivity increases with the increase of the initial crack length no matter where the current is injected. The difference in current injection position has a significant effect on the signal sensitivity. The sensitivity of the potential difference signal is greatest when the current injection point is near the upper left corner of the specimen.

Table 1 shows the average sensitivity gain at different initial crack lengths based on the average sensitivity at  $a_0/W=0.35$ . It can be seen that there is a significant difference in sensitivity with different initial crack lengths. In addition, the closer the current input point is to the upper right corner of the specimen, the more obvious the influence of the initial crack length on the sensitivity.

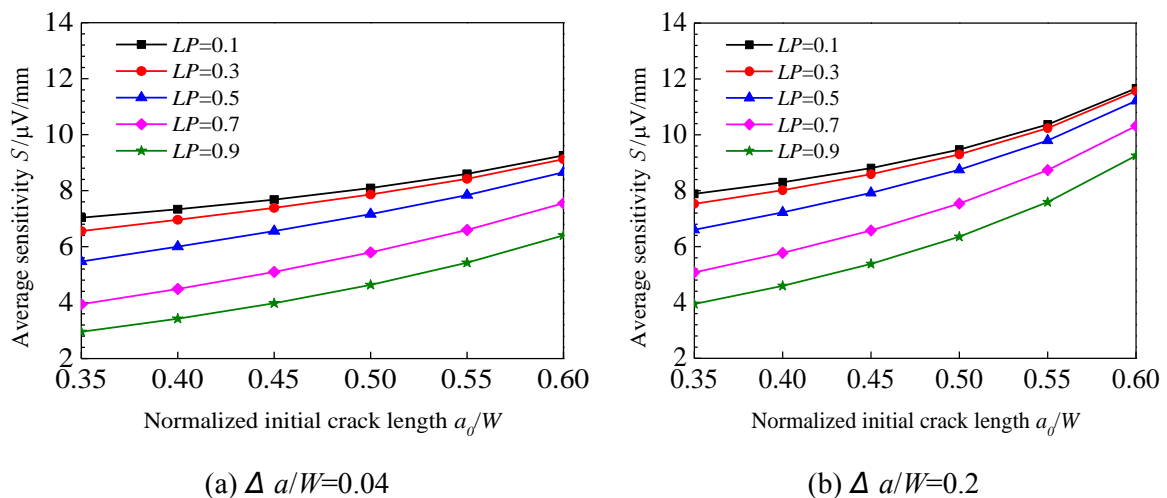


**Figure 4.** The average sensitivity for two crack extension ranges

**Table 1.** The average sensitivity gain (%) based on the average sensitivity at  $a_0/W=0.35$

	$a_0/W$				
	0.4	0.45	0.50	0.55	0.6
$LP=0.1$	5.2	11.7	20.1	31.4	47.8
$LP=0.3$	6.5	14.1	23.5	36.0	53.6
$LP=0.5$	9.4	20.0	32.6	48.4	69.9
$LP=0.7$	13.7	29.6	48.6	72.2	103.3
$LP=0.9$	16.5	36.4	61.1	92.5	134.6

3.2. Linearity

Figure 5 (a) and (b) show the  $\Delta U-\Delta a/W$  curves for different initial crack lengths at two current injection positions. As can be seen from the figures, the linearity of the  $\Delta U-\Delta a/W$  curve is different for different initial crack lengths. The larger the initial crack length, the worse the linear characteristic. Figure 6 (a) and (b) show the  $\Delta U-\Delta a/W$  at different current injection positions for two initial crack lengths. It can be seen from the figures that the current input position also has a significant influence on the linearity of the  $\Delta U-\Delta a/W$  curve. The closer the current input point is to the upper right corner of the specimen, the worse the linearity. For quantitative observations, all the  $\Delta U-\Delta a/W$  curves for different initial crack lengths and different current input positions were linearly fitted using the end-base method, and the linearity was then calculated. The results are shown in Table 2.

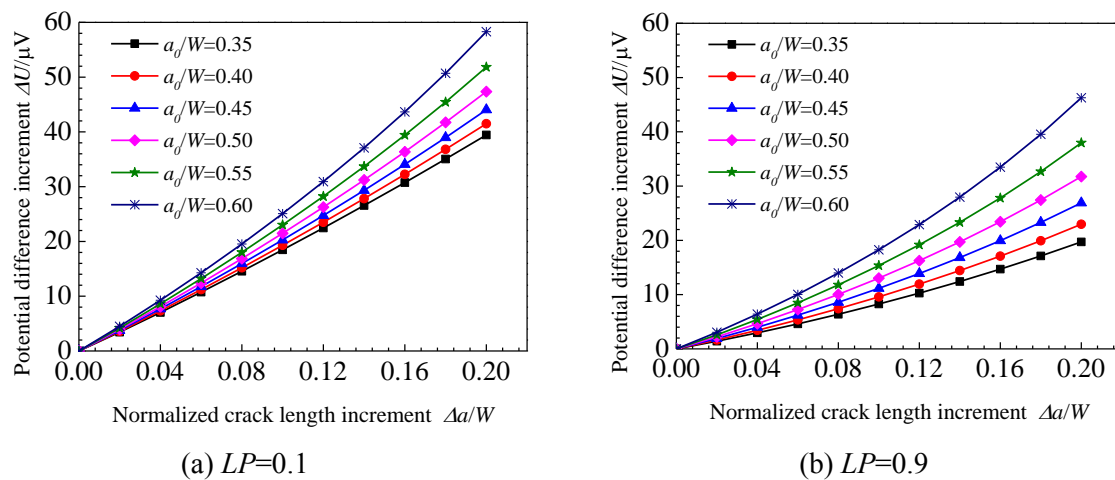


Figure 5. The  $\Delta U-\Delta a/W$  curves for two current injection positions

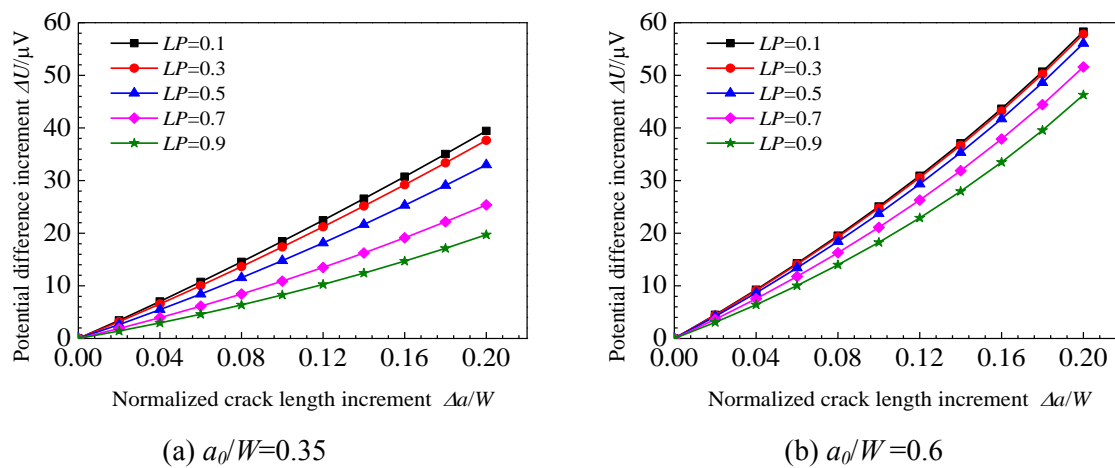


Figure 6. The  $\Delta U-\Delta a/W$  curves for two initial crack length

Table 2. The linearity(%) with different initial crack length and different current injection positions

	$a_0/W$					
	0.35	0.4	0.45	0.50	0.55	0.6
$LP=0.1$	3.2	3.5	4.0	4.6	5.6	7.0
$LP=0.3$	3.8	4.0	4.3	4.9	5.8	7.2
$LP=0.5$	5.2	5.2	5.4	5.8	6.5	7.7

$LP=0.7$	7.0	7.1	7.2	7.5	8.1	9.1
$LP=0.9$	8.1	8.3	8.5	8.9	9.6	10.5

#### 4. Conclusions

The initial crack length of the C(T) specimen has a significant influence on the sensitivity of the potential difference signal and the linearity of the potential difference-crack length curve. Selecting a larger initial crack length can increase the signal sensitivity. However, as the initial crack length increases, the linearity of the potential difference-crack length curve becomes worse.

#### Acknowledgments

This work is financially supported by the National Natural Science Foundation of China (Grant nos. 51475362, 51775427, and 11502195), the Key Research and Development Project of Shaanxi Province (grant no. 2017GY-034) and the Ph.D. Research Fund Project of Xi'an University of Science and Technology (grant no. 2018QDJ009)

#### References

- [1] Jia X, Xu-Teng HU, Song Y D. Calculation Formula for Stress Intensity Factors of CT Specimens based on Three Dimensional Finite Element Solutions[J]. Materials for Mechanical Engineering, 2015.
- [2] Yao Y, Cai L, Bao C, et al. Fracture Toughness Based on Test Method for Straight-Notch CT Specimen[J]. Journal of Aeronautical Materials, 2014, 34(6):67-74.
- [3] Xue H, Sato Y, Shoji T. Quantitative Estimation of the Growth of Environmentally Assisted Cracks at Flaws in Light Water Reactor Components[J]. Journal of Pressure Vessel Technology, 2009, 131(1) : 011404.
- [4] Dong-Hai D U, Kai C, Lun Y U, et al. Measurement of Fatigue Crack Growth Rate of Reactor Structural Material in Air Based on DCPD Method[J]. Atomic Energy Science & Technology, 2014, 48(8):1386-1391.
- [5] Wang L, Ding C F. Application of DC Current Method for Crack Length Measurement in High Temperature[J]. Journal of Aeronautical Materials, 2006, 26(3):359-360.
- [6] Ritchie R O, Bathe K J. On the calibration of the electrical potential technique for monitoring crack growth using finite element methods[J]. International Journal of Fracture, 1979, 15(1):47-55.
- [7] Johnson H H. Calibrating the electric potential method for studying slow crack growth[J]. Materials Research And Standards, 1965, 5: 442-445.
- [8] Chen Chi. Metal Fracture Research Collection [M]. Beijing: Metallurgical Industry Press, 1978. 113-114.
- [9] Z.J. Li, H. Xue. Numerical calibration of crack monitor based on direct current potential drop[J]. Journal of Xi'an University of Science and Technology, 2012, 32(1):116-116.
- [10] ASTM E399-09, Standard Test Method for Linear-Elastic Plane-Strain Fracture Toughness  $K_{Ic}$  of Metallic Materials[S], 2009.